Earth and Planetary Science Letters 617 (2023) 118237

Contents lists available at ScienceDirect

Earth and Planetary Science Letters

journal homepage: www.elsevier.com/locate/epsl

Reconciling biogeochemical redox proxies: Tracking variable bottom water oxygenation during OAE-2 using vanadium isotopes

Siqi Li [a,*], Oliver Friedrich [b], Sune G. Nielsen [c], Fei Wu [d], Jeremy D. Owens [a]

[a] Department of Earth, Ocean and Atmospheric Science, Florida State University and National High Magnetic Field Laboratory, Tallahassee, FL, USA
[b] Institute of Earth Sciences, Heidelberg University, Heidelberg, Germany
[c] Department of Geology and Geophysics, Woods Hole Oceanographic Institution, Woods Hole, MA, USA
[d] School of Earth Sciences, State Key Laboratory of Geological Processes and Mineral Resources, China University of Geoscience, Wuhan, Hubei, China

ARTICLE INFO

Article history:
Received 21 February 2023
Received in revised form 19 May 2023
Accepted 22 May 2023
Available online xxxx
Editor: A. Jacobson

Keywords:
sedimentary V isotope compositions
short-term bottom water oxygenation
bottom water redox fluctuations
oceanic anoxic event-2

ABSTRACT

Oceanic Anoxic Event-2 (OAE-2, ~94 Ma ago) is marked by a significant perturbation to the carbon and nutrient cycles. Despite the general idea of widespread expansion of the oceanic anoxia during OAE-2, various localities likely experienced heterogeneous redox fluctuations throughout the roughly 500-thousand-year-long event. In certain localities, redox-sensitive elements imply persistent anoxic-to-euxinic conditions, notwithstanding paleontological data that indicate short-term hypoxic-to-anoxic oscillations in bottom waters. Such discrepancies likely result from sampling resolution, local proxy sensitivity, and/or time-integration of signals, particularly for severe hypoxic conditions. We applied vanadium (V) isotopes to three well-studied OAE-2 localities in the proto-North Atlantic Basin. Under the relatively stable anoxic-to-euxinic conditions throughout OAE-2 at Well S75 and Site 367, the sedimentary δ^{51}V values present consistent variations analogous to modern anoxic-to-euxinic environments. However, at Site 1258, the sedimentary δ^{51}V values present greater perturbations toward more negative values that are indicative of short-term oxygenation in bottom waters. These negative perturbations of δ^{51}V values covary with the abundances of the low-oxygen-tolerant benthic foraminifers. Together, these data refine the heterogeneous redox fluctuations in individual localities, revealing occasional short-term weak oxygenation under the generally anoxic conditions throughout OAE-2. This study documents the unique utility of V isotopes to track bottom water redox fluctuations, particularly short-term variations from anoxic to mildly oxic conditions that are hard to track with other methods.

1. Introduction

Punctuated expansions of oxygen-deficient or even completely absent (anoxic) conditions over the seafloor in the Mesozoic, which have been termed as oceanic anoxic events (OAEs), have remarkably perturbed the carbon and nutrient cycling, and the marine biological evolutions (e.g., mass extinction events). Oceanic Anoxic Event-2 in the Late Cretaceous (OAE-2, ~94 Ma ago) is one of the best-studied and globally recognized OAEs in the Phanerozoic and is conventionally constrained by an abrupt positive carbon isotope excursion (CIE) of both organic and carbonate carbon isotopes (e.g., Kuypers et al., 2002; Erbacher et al., 2005; Kolonic et al., 2005; Elrick et al., 2009). These data have been attributed to the massive sedimentary burial of ^{12}C-enriched organic matter promoted either by primary productivity due to increased nutrient availability (Adams et al., 2010; Owens et al., 2012; Pogge von Strandmann et al., 2013; Du Vivier et al., 2014) or by the expansion of oxygen-deficient, carbon burial-conducive conditions over the seafloor (e.g., Jenkyns, 2010; Owens et al., 2016; Ostrander et al., 2017).

The application of geochemical proxies, e.g., Tl isotopes (Ostrander et al., 2017), trace metal enrichment (Owens et al., 2016), has proposed an expansion of global anoxic (oxygen-absent but non-sulfidic) conditions over the seafloor before the initial carbon cycle perturbation. Additionally, sulfur isotope compositions of carbonate-associate sulfate (Owens et al., 2013) and Mo isotope compositions of black shales (Westermann et al., 2014; Dickson et al., 2016) suggest that euxinic (sulfidic water columns) conditions expanded globally nearly coincident with the CIE. In contrast, the local redox conditions were more spatiotemporally variable, which makes it more difficult to untangle local effects and impacts of OAE-2 (e.g., Kuypers et al., 2002; Kuhnt et al., 2005; Poulton et al., 2015; Owens et al., 2016). Enrichment of redox-sensitive elements (RSEs) such as V, U, and Mo in sediments has been

* Corresponding author.
E-mail address: sli8@fsu.edu (S. Li).

https://doi.org/10.1016/j.epsl.2023.118237
0012-821X/

utilized to constrain local depositional redox conditions and, potentially, the global redox responses (e.g., Algeo, 2004; Tribovillard et al., 2006; Owens et al., 2016). To independently constrain the local redox conditions, sedimentary Fe proxies have been investigated to constrain local anoxic, ferruginous, and euxinic conditions (Lyons and Severmann, 2006; Poulton and Canfield, 2011). However, trace metal redox geochemical proxies can also be affected by sedimentation rates, changes in lithology (e.g., the proportion of detrital silicates and biogenic materials), and/or post-depositional processes (Lyons and Severmann, 2006; Tribovillard et al., 2006; Scholz et al., 2011; Cole et al., 2017; Raiswell et al., 2018; Liu and Algeo, 2020). Over the last few decades, non-traditional stable metal isotopes, especially uranium isotopes (Clarkson et al., 2018; Zhang et al., 2020) and molybdenum isotopes (Dickson et al., 2016; Dickson, 2017; Kendall et al., 2017), have been implemented to constrain local and/or global oceanic anoxia and euxinia. These proxies can provide a window into the dominant anoxic/euxinic conditions for a given locality and are effective at documenting redox changes farther down the redox ladder such as Fe reduction to sulfate reduction, but have limited capability to constrain the oxygen-deficient conditions. Importantly, the zone of severe oxygen depletion termed as hypoxic-to-anoxic conditions in this work can cause mass mortality at or below 22 μM of dissolved [O_2] as suggested by modern biology, and suppress bioturbation, therefore sediment ventilation, which in turn affects the nutrient cycling at the sediment-seawater interface (Levin et al., 2009; Middelburg and Levin, 2009; Hofmann et al., 2011; Sturdivant et al., 2012). However, this oxygen-deficient zonation remains ambiguous regardless of current geochemical proxies (previous V isotope work suggests it responds near 10 μM of dissolved [O_2]; Wu et al., 2020) and is difficult to reconstruct in the ancient oceans due to discrepancies between geochemical and paleontological evidence (e.g., Boyer et al., 2011).

For Ocean Drilling Program (ODP) Site 1258, the authigenic enrichment of RSEs including Fe speciation data suggests that this site was predominantly euxinic throughout OAE-2 (Owens et al., 2016). This, however, presents some discrepancies with published paleontological records (Friedrich et al., 2006; Berrocoso et al., 2008) that show the occurrence of benthic organisms with low oxygen requirements in discrete horizons during OAE-2, which implies short-term increases of bottom water oxygenation at this site. So far, these discrepancies have not been addressed as there are limited geochemical proxies sensitive enough to track the hypoxic-to-anoxic fluctuations, especially for geologically short-time intervals. Importantly, the widespread expansion of the hypoxic-to-anoxic conditions likely was a precursor for many reducing events in the geologic record such as OAEs and mass extinction events but currently is under-constrained due to limited geochemical specificity. Recent research on the sedimentary V isotope system in modern oceans has revealed a strong dependence of V isotope ratios on bottom water redox fluctuations, particularly across the transition from anoxic to severe hypoxic in bottom waters (Wu et al., 2020). There is, therefore, the potential for V isotopes, in conjunction with other biogeochemical tools, to provide better constraints on the spatiotemporal redox structures in ancient oceans (Fan et al., 2021; Heard et al., 2023; Wei et al., 2023).

As a novel redox proxy, sedimentary V isotope compositions are proposed to be able to track the redox fluctuations in bottom waters based on observations in modern marine sediments deposited under different redox conditions (Wu et al., 2020). Dissolved V is dominated by V(V) species $H_2VO_4^-$ and HVO_4^{2-} in modern oxic oceans, with a concentration range of ~35-45 nM and a relatively long residence time of ~90 kyrs (thousand years; as reviewed in Nielsen, 2020). The relatively short residence time in comparison with U (400-500 kyrs, Zhang et al., 2020 and reference therein) and Mo (~440 kyrs, Kendall et al., 2017 and reference therein) suggests a more rapid response of the marine V isotope system to climate perturbations such as geologically short-lived OAEs. Vanadium generally behaves as a conservative element in open oceans albeit there is a minor depletion observed in surface seawater due to adsorption or biological scavenging (Collier, 1984; Ho et al., 2018). The main input of V to the ocean system is the riverine flux mainly derived from silicate weathering (Shiller and Mao, 2000). The output mainly includes sediments deposited under different redox environments and hydrothermal systems (as reviewed in Nielsen, 2020 and reference therein). In oxic environments, V(V) is scavenged by Fe and Mn oxyhydroxides, resulting in enrichment in pelagic sediments with significant components of these minerals (e.g., Trefry and Metz, 1989; Ho et al., 2018; Wu et al., 2019b; Li et al., 2021). As the depositional environments evolve to oxygen-deficient conditions, V(V) can be reduced to V(IV) which is prone to be adsorbed onto or incorporated into sinking particulates or organic ligands (Lewan and Maynard, 1982; Wehrli and Stumm, 1989; Wang and Sañudo Wilhelmy, 2009; Ho et al., 2018; Knežević et al., 2021). Vanadium has two stable isotopes, ^{51}V (99.76%) and ^{50}V (0.24%), and the isotope composition is expressed by the following formula:

$$\delta^{51}\,V_{sample}\,(‰) = \left(\frac{^{51/50}V_{sample}}{^{51/50}V_{standard}} - 1\right) \times 1000 \qquad (1)$$

The pure V solution from Alfa Aesar Chemicals (AA-V) is utilized as the analytical standard and its value is arbitrarily set to 0‰ (Nielsen et al., 2011). Theoretical calculations predict pronounced isotope fractionations among different V species during physicochemical processes (Wu et al., 2015), which is also testified by recent data in modern marine sediments (Wu et al., 2019b; Wu et al., 2020). Up to date, V isotope data suggest that the open oceans have relatively homogeneous $\delta^{51}V$ values with an average value of 0.20 ± 0.07‰ (2SE, Schuth et al., 2019; Wu et al., 2019a; Nielsen, 2020). Compared with the seawater $\delta^{51}V$ values, marine sediments are characterized with more negative $\delta^{51}V$ values. Core-top sediments deposited under the stable euxinic conditions in the Cariaco Basin are characterized by the most positive authigenic $\delta^{51}V$ values among all the sinks with an average value of -0.22 ± 0.05‰ (2SE, Nielsen, 2020; Wu et al., 2020), presenting the smallest isotopic difference to seawater ($\Delta_{sw\text{-}euxinic} = \delta^{51}V_{sw} - \delta^{51}V_{euxinic}$, "sw" denotes seawater) of ~0.42‰. In contrast, sediments deposited under anoxic conditions (literally defined as the absence of dissolved O_2 whereas operationally defined as the dissolved [O_2] lower than the limit of determination, LOD) present relatively more negative authigenic $\delta^{51}V$ values with an average value of -0.46 ± 0.06‰ (2SE, LOD of dissolved [O_2] is ~2 μM. Scholz et al., 2011; Nielsen, 2020; Wu et al., 2020) and the $\Delta_{sw\text{-}anoxic}$ ($\Delta_{sw\text{-}anoxic} = \delta^{51}V_{sw} - \delta^{51}V_{anoxic}$) is ~0.66‰. For sediments deposited in oxic conditions (pelagic sediments and oxic sediments deposited on continental margin areas), the average value of authigenic sedimentary $\delta^{51}V$ values is -0.90 ± 0.04‰ (2SE, Nielsen, 2020; Wu et al., 2020), and the $\Delta_{sw\text{-}oxic}$ ($\Delta_{sw\text{-}oxic} = \delta^{51}V_{sw} - \delta^{51}V_{oxic}$) is ~1.10‰. Observations in various depositional environments in modern ocean basins suggest redox conditions as the dominant factor controlling the authigenic sedimentary V isotopic signatures with limited alterations from post-depositional diagenesis (Wu et al., 2020; Chen et al., 2022), although future research probing the potential influence from early diagenesis is required. Moreover, despite the limited correlation between the authigenic sedimentary $\delta^{51}V$ compositions and the variable sedimentation rates as observed along the Peruvian margin OMZ area (Wu et al., 2020), noteworthily, the isotopically-disequilibrated dynamic processes involving fast and

efficient uptake of V from ambient seawater by sinking particulates in a hydrothermal buoyant plume (Wu et al., 2022) could also shift the particulate δ^{51}V signature toward seawater endmember. Therefore, the substantial variations of the authigenic sedimentary δ^{51}V values should document coupled information of the local depositional environments and the coeval seawater δ^{51}V values (see further discussion below).

Under steady-state conditions, the seawater δ^{51}V value is controlled by the relative proportions of sinks with different isotopic signatures, assuming a constant riverine δ^{51}V value as illuminated by the equation (2):

$$\delta^{51}V_{sw} = \delta^{51}V_{river} + \sum f_i \cdot \Delta_{sw-sink_i} \quad (2)$$

where "sw" denotes seawater and "i" denotes a certain sink that can be oxic, anoxic, euxinic, and hydrothermal. The f_i is the fraction of sink$_i$ ($\sum f_i = 1$). The $\Delta_{sw-sink_i}$ $\left(\delta^{51}V_{SW} - \delta^{51}V_{sink_i}\right)$ is the isotopic difference between seawater and sink$_i$. Based on the modern V isotope mass balance, the increased burial of V in anoxic and euxinic environments can result in a significant negative shift of seawater δ^{51}V values (Nielsen, 2020). The overall shift for seawater is ~0.4‰ (assuming consistent isotopic fractionation factors based on modern marine observations), and such a magnitude would require a large expansion of euxinic environments (Nielsen, 2020; Fan et al., 2021; Heard et al., 2023; Wei et al., 2023). Thus, V isotope compositions in ancient marine sediments can both reflect changes in local redox conditions as indicated by relatively short-term fluctuations or variations of the seawater V isotope compositions as indicated by the systematic shifting of the sedimentary δ^{51}V profiles.

In this study, we applied V isotopes to OAE-2 and determined the sedimentary δ^{51}V values of organic-rich sediments spanning this perturbation from three sites in the proto-North Atlantic Basin. The local redox conditions of these localities throughout OAE-2 are relatively well studied with geochemical and/or biological proxies (e.g., Kuypers et al., 2002; Kuhnt et al., 2005; Friedrich et al., 2006; Owens et al., 2016; Raven et al., 2019), thus providing a robust framework to test the responses of the V isotope system to the local inter- and intra-site variabilities of redox conditions and the global expansion of oceanic anoxia.

2. Geologic setting

We studied three sites in the proto-North Atlantic Basin with the OAE-2 section being marked by the positive CIE: Well S75 in the Tarfaya Basin, Deep Sea Drilling Program (DSDP) Site 367 in the southeastern tropical North Atlantic and Ocean Drilling Program (ODP) Site 1258 on the Demerara Rise (Fig. 1). Well S75 is located in the Tarfaya Basin and benthic fossil assemblages indicate a continental shelf setting with a paleodepth of ~200-300 m in the Late Cretaceous (Einsele and Wiedmann, 1982; Kuhnt et al., 1997). Sediments in the Tarfaya Basin throughout OAE-2 mainly present alternating layers of organic-rich, dark-colored, finely laminated marlstones with high total organic carbon contents (TOC% ranging from ~2% to > 10%) and organic-poor, light-colored, homogeneous limestones (Kuhnt et al., 1997; Kolonic et al., 2005; Kuhnt et al., 2005). DSDP Site 367 is located off the coast of northwest Africa with a paleodepth of ~3700 m in the Late Cretaceous (Kuypers et al., 2002). The local lithology throughout OAE-2 is dominated by finely laminated black shales devoid of fossils (Sinninghe Damsté and Köster, 1998). The occurrence of a hiatus in the upper portion of the CIE does not allow to constrain the duration and termination of OAE-2 at this site. For the remaining interval, the average TOC% value sharply increases from ~8.5% prior to OAE-2 to ~24.6% during OAE-2. Such high TOC% values are mainly attributed to the local high primary productivity boosted by enhanced nutrient supplies (Kuypers et al., 2002). ODP Site 1258 is located on the northwestern slope of the Demerara Rise. The northern edge of the Demerara Rise subsided to a paleodepth of ~2000 m in the Late Cenomanian (Erbacher et al., 2004). Sediments throughout OAE-2 are mainly dominated by organic-rich, laminated black shales (TOC% ranging from 2% to 29%) which we aimed for this work but there are occasional thin layers of light-colored, laminated foraminiferal packstones and wackestones (Erbacher et al., 2005; Friedrich et al., 2006).

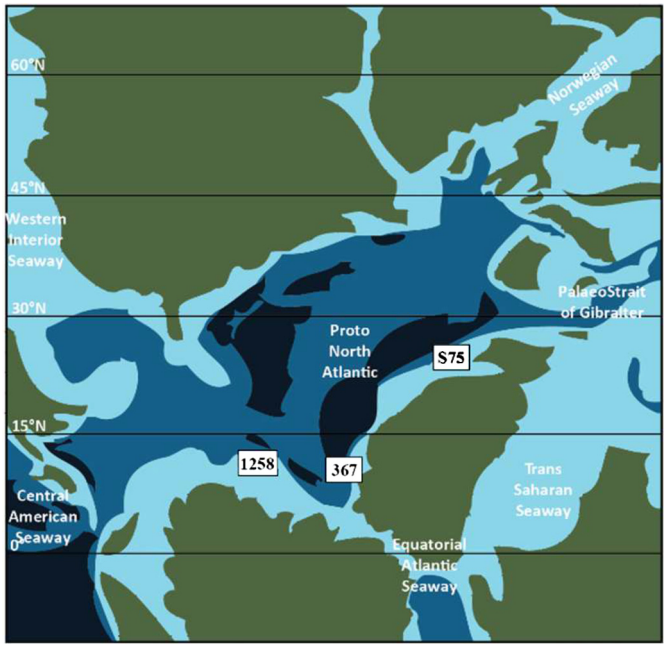

Fig. 1. Map of the proto-North Atlantic Basin in the Late Cretaceous (modified from Owens et al. (2012)). The green color marks the subaerial continents and the blue gradients denote the depth of the marine settings with deeper depth indicated by darker blue color.

3. Materials and methods

3.1. Elemental concentrations

All the samples were ashed under ~550 °C in the furnace overnight to remove organic matter and then bulk digested with double-distilled trace-metal-clean HF-HNO_3-HCl mixed acid. Bulk Al and V concentrations for samples at Well S75 were measured with Agilent 7500ce ICP-MS (Table S1), with the relative standard deviation (RSD) < 6% for Al and < 2% for V. The shale standard SGR-1 was utilized to monitor the precision of ICP-MS, and the Al and V concentrations are 3.38 ± 0.20% and 128 ± 3 ppm respectively, in agreement with certified values of 3.45 ± 0.11% (1SD) for Al and 130 ± 6 ppm (1SD) for V (USGS Reference Material Information Sheet). Determination of elemental concentrations for samples at Site 367 was completed and the method was described in earlier work (Owens et al., 2012, Table S2). Elemental concentrations for samples at Site 1258 are from Owens et al. (2016) and are presented in Table S3. Despite the considerable background abundance of V in detrital silicates, the potential bias between the authigenic and bulk V isotopic values ($\Delta^{51}V_{auth-bulk} = \delta^{51}V_{auth} - \delta^{51}V_{bulk}$) due to the bulk digestion method is dependent on the proportion of authigenic V (f_{auth}), and the isotopic difference between the detrital V and the bulk V ($\Delta^{51}V_{bulk-detri} = \delta^{51}V_{bulk} - \delta^{51}V_{detri}$):

$$\Delta^{51}V_{auth-bulk} = \left(\frac{1}{f_{auth}} - 1\right) \cdot \Delta^{51}V_{bulk-detri} \quad (3)$$

For the sample with the lowest V enrichment factor (V_{EF} = $(V/Al)_{sample}$ / $(V/Al)_{average\ upper\ continental\ crust\ (UCC)}$, the Al and V contents of the average UCC are referred to Rudnick and Gao (2003)) of 6, the potential isotopic bias from detrital silicates is ~0.10‰, within the long-term analytical precision in our lab (see following discussion in 3.2. Vanadium isotope compositions), assuming the $\delta^{51}V$ value of the average UCC similar to the runoff value of ~-0.70‰ (Schuth et al., 2019) due to non-significant isotopic fractionation of V isotopes during the chemical weathering (Qi et al., 2022).

3.2. Vanadium isotope compositions

A four-column ion exchange chromatography method was adopted to extract and purify V and the specific procedures were established and refined in earlier work (Nielsen et al., 2011; Wu et al., 2016). In general, the Bio-Rad AG 50W-X12 (200-400 mesh) cation resin was utilized to remove matrix elements. As ^{50}Ti and ^{50}Cr can substantially interfere with ^{50}V signal, the Bio-Rad AG1-X8 (200-400 mesh) chloride-form anion resin was utilized to quantitatively remove remnant trace Ti and Cr. Determination of V isotope compositions was completed with Neptune Multicollector-Inductively Coupled Plasma Mass Spectrometer and the instrument settings are described in detail by Nielsen et al. (2016) except that the $10^{11}\Omega$ resistor was employed for the center cup to collect ^{50}V signal. Because V only has two stable isotopes, we utilized the sample-standard bracket method to monitor the instrument stability. Alfa Aesar pure V solution (AA-V) was utilized as the reference solution and V isotope compositions of samples are expressed as $\delta^{51}V_{Sample}$ (‰) = $(^{51/50}V_{Sample}/^{51/50}V_{AA} - 1) \times 1{,}000$. Pure BDH V standard solution (BDH-V, VWR Chemical BDH) was utilized to monitor the long-term in-lab precision and was run before and after each sample. The average value of BDH-V is -1.18 ± 0.11‰ (2SD, n = 797), in agreement with previously published data (Nielsen et al., 2011; Wu et al., 2016). Values of shale standards SGR-1 and SDO-1 are -0.25 ± 0.09‰ (2SD, n = 21) and -0.56 ± 0.07‰ (2SD, n = 5) respectively, consistent with earlier published datasets of -0.21 ± 0.11‰ and -0.54 ± 0.11‰ (Wu et al., 2020).

3.3. Benthic foraminifers

Samples were cleaned and processed in earlier work (Friedrich et al., 2006) which were different subsets of samples from the presented geochemical data. The abundance and diversity of benthic foraminifers was investigated from >63 μm portion. In this study, the low-oxygen-tolerant benthic foraminifera taxa, *Gavelinella spp.* (Herrle et al., 2003; Friedrich et al., 2005), are utilized as independent paleontological evidence to track the transient recovery to weak oxygenation in bottom waters throughout OAE-2 at Site 1258 (Table S4).

4. Results and discussion

The sedimentary V_{EF} and $\delta^{51}V$ values are presented in Tables S1, S2, and S3, and are plotted in Fig. 2. The three sites present variable enrichment degrees of authigenic sedimentary V with V_{EF} varying between 7-48, 8-81, and 6-93 at Well S75, Site 367, and Site 1258 respectively. The high V_{EF} values should indicate generally strongly reducing conditions at the three sites throughout OAE-2, whereas such temporospatial variabilities of V enrichment degrees in sediments should reflect complex influence from depositional factors such as the local redox fluctuations, the lithology variabilities (fluxes of organic matter, carbonates, and detrital silicates), and the sedimentation rates (Kuypers et al., 2002; Erbacher et al., 2005; Kolonic et al., 2005; Kuhnt et al., 2005; Owens et al., 2016). The sedimentary $\delta^{51}V$ profiles at Well S75 and Site 367 present a consistent fluctuation range throughout OAE-2. At Well S75, the sedimentary $\delta^{51}V$ values vary between -0.46‰ to -0.28‰ prior to OAE-2 and between -0.44‰ to -0.18‰ for the OAE-2 section. Promptly following OAE-2, the sedimentary $\delta^{51}V$ values present a similar range of -0.47‰ to -0.16‰ despite one point with a more negative value of -0.60‰ (Fig. 2A). For Site 367, the pre- and initial-portion of OAE-2 is well preserved and the sedimentary $\delta^{51}V$ values vary between -0.44‰ to 0.08‰ and between -0.36‰ to -0.04‰, respectively (Fig. 2B). However, the sedimentary $\delta^{51}V$ values for the mid-to-late portion of OAE-2 cannot be constrained due to the lack of sedimentary recovery at this site. The sedimentary $\delta^{51}V$ values at Site 1258 vary between -0.72‰ and -0.21‰ prior to OAE-2, and such sedimentary $\delta^{51}V$ fluctuations narrow slightly within a range of -0.57‰ to -0.22‰ during the OAE-2 portion and -0.28‰ to -0.23‰ following the event (Fig. 2C). All three sites present fluctuating sedimentary $\delta^{51}V$ profiles throughout OAE-2 that do not appear correlated with the age relative to the CIE (Fig. 2). To the first order, the V isotope fluctuations, therefore, likely reflect variable local redox conditions during deposition at the three sites. However, superimposed upon these local effects could be V isotope variations of seawater itself, which is further discussed in our interpretations. It is important to note that due to the current analytical limitation of the sedimentary V isotope methodology (Wu et al., 2020) and the extremely low V concentrations in biogenic carbonates (< 0.1 ppm V in clean foraminiferal calcite, Hastings et al., 1996), we did not analyze V isotope compositions for the homogeneous light-colored, organic-poor limestone layers at Well S75, although Dong et al. (2021) has analyzed carbonate samples.

4.1. OAE-2 seawater $\delta^{51}V$ values

Despite the general global widespread oceanic anoxia during OAE-2, the three sites presented variable local redox conditions throughout this event. Well S75 was characterized with repetitive millennial-scale oscillations of the depositional conditions throughout OAE-2 as expressed by the rapidly alternating lithology and the abundances of benthic foraminifers (Kuhnt et al., 2005), however, we only analyzed the dark-colored, organic-rich lithologies. The homogeneous light-colored, organic-poor limestone intervals contain more abundant and diverse benthic foraminifers, which indicates more oxic conditions allowing for the proliferation of benthos (Kuhnt et al., 2005). In contrast, the finely laminated organic-rich, dark-colored intervals present anoxic-to-euxinic conditions as indicated by the lack of benthic foraminifers (Kuhnt et al., 2005), the enrichment of redox-sensitive trace metals (V, Zn, and Mo) and the increased burial of biomarkers (isorenieratene and chlorobactene) (Kolonic et al., 2005). For Site 367, the finely laminated organic-rich black shales absent of benthic fauna and the highly enriched sedimentary V and Mo indicate the development of anoxic-to-euxinic conditions in bottom waters prior to OAE-2 (Kuypers et al., 2002). The enhanced preservation of molecular biomarkers (isorenieratene and chlorobactene) synchronous with the initiation of the CIE proposes the development of photic zone euxinia during OAE-2 (Kuypers et al., 2002). The Fe speciation at Site 367 also generally suggests anoxic-to-euxinic bottom waters prior to OAE-2 and intensified euxinic conditions during the event (Westermann et al., 2014), which suggests consistency in the interpretation of previous trace metal and biological evidence. Thus, the geochemical and biological data from Well S75 and Site 367 are in agreement. However, at Site 1258, there is some disagreement between the published geochemical and paleontological evidence constraining the local redox fluctuations. The sedimentary Fe speciation (Owens et al., 2016) and elevated burial of organic matter with high S/C ratios (Raven et al., 2019) indicate local persistent eux-

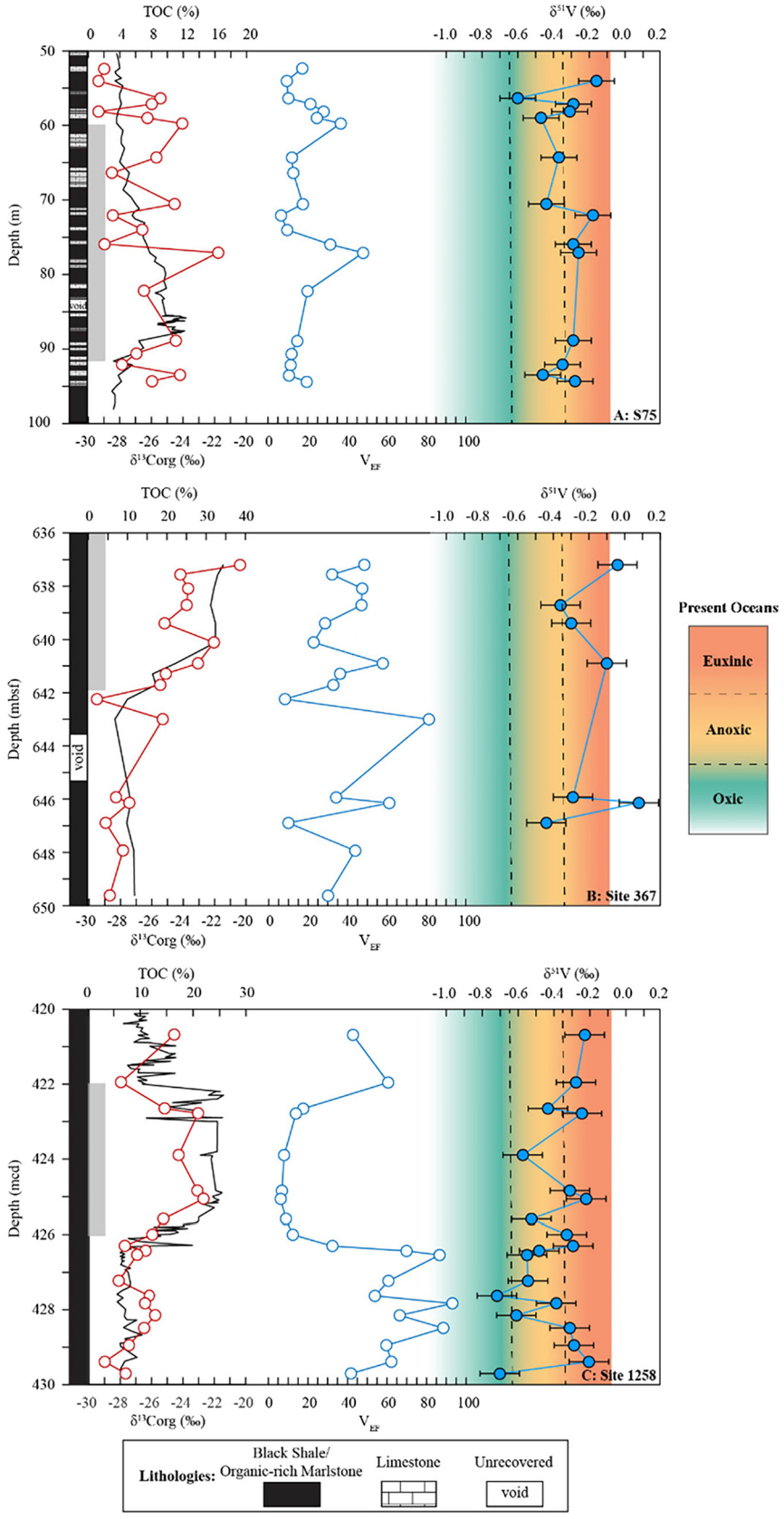

Fig. 2. The sedimentary profiles of TOC (red circles and lines), organic carbon isotopic compositions (δ^{13}Corg, black line), V_{EF}, and δ^{51}V at Well S75, DSDP Site 367, and ODP Site 1258. The long-term 2SD of 0.11‰ is applied to δ^{51}V values if the sample 2SD is less than that. The grey bar indicates the duration of OAE-2 as constrained by the positive CIE. The TOC data at S75, Site 367, and Site 1258 are respectively from Kuhnt et al. (2005), Kuypers et al. (2002), and Owens et al. (2012). The δ^{13}Corg data at S75, Site 367, and Site 1258 are respectively from Kuhnt et al. (2005), Kuypers et al. (2002), and Erbacher et al. (2005). The sedimentary Al and V concentrations at Site 1258 are from Owens et al. (2016). The color bar indicates the characteristic authigenic sedimentary δ^{51}V ranges documented in different redox environments in modern oceans (Nielsen, 2020; Wu et al., 2020).

inic conditions shoaling upward into the shallower water columns; however, the occasional occurrence of benthic foraminifers suggests short-term oxygenation, albeit minimal, in bottom waters, which appeared more frequently for the pre-OAE-2 portion of the section (Friedrich et al., 2006).

A significant reduction of the oceanic V reservoir size due to the intensive expansion of the oceanic anoxia was previously proposed (Owens et al., 2016 and reference therein), which, meanwhile, may result in perturbations to the contemporaneous seawater δ^{51}V values (Nielsen, 2020; Fan et al., 2021; Heard et al., 2023; Wei et al., 2023). However, despite the predominantly local anoxic-to-euxinic conditions throughout the analyzed section of Site 367 and the organic-rich intervals at Well S75, such a Rayleigh-type correlation between the sedimentary V concentrations and the sedimentary δ^{51}V values (e.g., Fan et al., 2021; Wei et al., 2023) is not observed as there is no trend or shift of the sedimentary δ^{51}V profiles. Instead, the sedimentary δ^{51}V values throughout OAE-2 have a range of values of −0.46‰ to −0.18‰ and −0.44‰ to 0.08‰ for Well S75 and Site 367, respectively, with rapid fluctuations of approximately 10 kyrs based on estimates using a linear sedimentation rate model (Kuypers et al., 2002; Kuhnt et al., 2005). Similar rapid fluctuations are not observed for Tl isotopes (Ostrander et al., 2017), which should record rapid global initial redox changes. Moreover, if we use the most positive sedimentary δ^{51}V values of the three sites as records under euxinic conditions and assume a consistent $\Delta_{\text{sw-euxinic}}$ value of 0.42‰, then the estimated seawater δ^{51}V values using data from Well S75, Site 367, and Site 1258 would be 0.24‰, 0.50‰ and 0.21‰, respectively. The extremely positive seawater δ^{51}V value of ∼0.50‰ based on the euxinic deposition at Site 367, based on the mass balance, is unlikely in a completely oxic ocean (Fan et al., 2021; Wei et al., 2023). Instead, the most positive value of ∼0.08‰ at Site 367 should result from the fast uptake of V by sinking particles from ambient seawater under strongly reducing conditions locally as indicated by the extremely high sedimentary V concentration of ∼4000 ppm (Fig. 3), alike in the hydrothermal systems (Wu et al., 2022). Furthermore, the most positive sedimentary δ^{51}V value at Site 367 also indicates that the contemporaneous seawater δ^{51}V values prior to OAE-2 cannot be less than the measured sedimentary archive of ∼0.08‰, which is analytically indistinguishable from modern seawater δ^{51}V range (Wu et al., 2019a). Except for this one value, the sedimentary δ^{51}V signatures at Site 367 and Well S75 present similar variations before and during OAE-2, proposing indiscernible shifting trend of contemporaneous seawater δ^{51}V signatures during this event.

We further test the potential feedback of the marine V reservoir size and the seawater δ^{51}V value to the intensive burial of V in the anoxic and/or euxinic environments during OAEs. A box model is adopted to investigate the responses of the global marine V reservoir (Algeo, 2004; Algeo and Lyons, 2006; Reinhard et al., 2013), the proportion of sinks (oxic, anoxic, euxinic, and hydrothermal), and the contemporaneous seawater δ^{51}V value to the enhanced burial of V in reducing environments due to the expansion of the oceanic anoxia and/or euxinia during OAEs. We start from the well-mixed global box model from the present dominantly oxic marine conditions (Table S5) and constrain the V outfluxes of specific sinks as a function of the area and the average burial rate in the sink (Reinhard et al., 2013), which is described with equation (4) and (5):

$$\frac{dM_V}{dt} = F_{ri} - \sum_{sink_i} F_i \tag{4}$$

$$F_i = \int_{A_i} b_i dA_i = A_i \cdot b_i \tag{5}$$

where M_V is the ocean V reservoir size (by mole). The F_{ri} denotes the influx, i.e., the riverine input. The F_i denotes the outflux for sink$_i$ where i can be oxic (ox), anoxic (an), euxinic (eu), and hydrothermal (hydr). The b_i is the average burial rate over the area of sink$_i$ (A_i), which is regulated by the seawater V concentration ([V], i.e., the marine V reservoir size) and the physicochemical processes removing V from ambient seawater characterized in sink$_i$ as illustrated by equation (6):

$$\mathrm{b_i} = [\mathrm{V}]^{\alpha_i} \cdot b_{i\_intri} \tag{6}$$

The b_{i_intri} represents the average intrinsic burial efficiency of sink$_i$, which is essentially controlled by the physicochemical processes removing V from ambient seawater in sink$_i$. As V is proposed to be mainly delivered to sediments by sinking particulates (Scholz et al., 2011; Wu et al., 2020), thus the characteristic b_{i_intri} in sink$_i$ should be mainly controlled by factors, for instance, the distributions of V species in different redox environments (Wanty and Goldhaber, 1992), the physicochemical properties of the sinking particulates (Fe and Mn oxides in oxic and hydrothermal environments, and organic particulates in reducing environments; as reviewed in Nielsen, 2020) and the particulate fluxes/precipitation rates (e.g., Scholz et al., 2011). In this modeling work, the average intrinsic burial efficiency is assumed consistent (i.e., the same as modern conditions) for all the sinks, namely, the average burial rate is partially regulated by the seawater [V]. This assumption is likely a simplification, but we are not quantifying the expansion of the anoxic/euxinic area. Instead, here we utilize this modeling work to discuss the potential feedback of the proportional distributions of different sinks, and the perturbations to the marine V reservoir size and the contemporaneous seawater δ^{51}V value due to the intensive elemental burial of V in anoxic/euxinic sinks along with the expansion of the oceanic anoxia/euxinia. This provides valuable understanding of the redox conditions but is more realistic given the current constraints on the V isotope system. The coefficient α_i reflects the controlling magnitude of the b_i from the seawater [V]. Therefore, the perturbation of the ocean V reservoir size can be described with equation (7):

$$\frac{dM_V}{dt} = F_{ri} - \sum_{sink_i} F_{i\_m} \cdot \frac{A_{i\_t}}{A_{i\_m}} \cdot \left(\frac{[V]_t}{[V]_m}\right)^{\alpha_i} \tag{7}$$

where the subscripts m and t, respectively, denote parameters prior to the expansion of the oceanic anoxia/euxinia (e.g., modern oxic oceans) and during the expansion of the oceanic anoxia/euxinia. Equation (7) can be converted to equation (8), assuming limited variations of the total seawater volume:

$$\frac{dM_V}{dt} = F_{ri} - \sum_{sink_i} F_{i\_m} \cdot \frac{A_{i\_t}}{A_{i\_m}} \cdot \left(\frac{M_{V\_t}}{M_{V\_m}}\right)^{\alpha_i} \tag{8}$$

Equation (8) allows the outfluxes to be primarily regulated by the sink area and the marine V reservoir size. It is important to note that the hydrothermal sink is calculated based on the hydrothermal fluid fluxes, the average Fe concentrations in the hydrothermal fluids, and the V/Fe ratios of hydrothermal sediments (Trefry and Metz, 1989; Nielsen, 2020), which is not further discussed here and is assumed to remain constant in the fluids, namely the $\frac{A_{hydr\_t}}{A_{hydr\_m}} = 1$.

When a new steady state is achieved,

$$\frac{dM_V}{dt} = 0 \tag{9}$$

$$F_{ri} = \sum_{sink_i} F_{i\_m} \cdot \frac{A_{i\_t}}{A_{i\_m}} \cdot \left(\frac{M_{V\_t}}{M_{V\_m}}\right)^{\alpha_i} \tag{10}$$

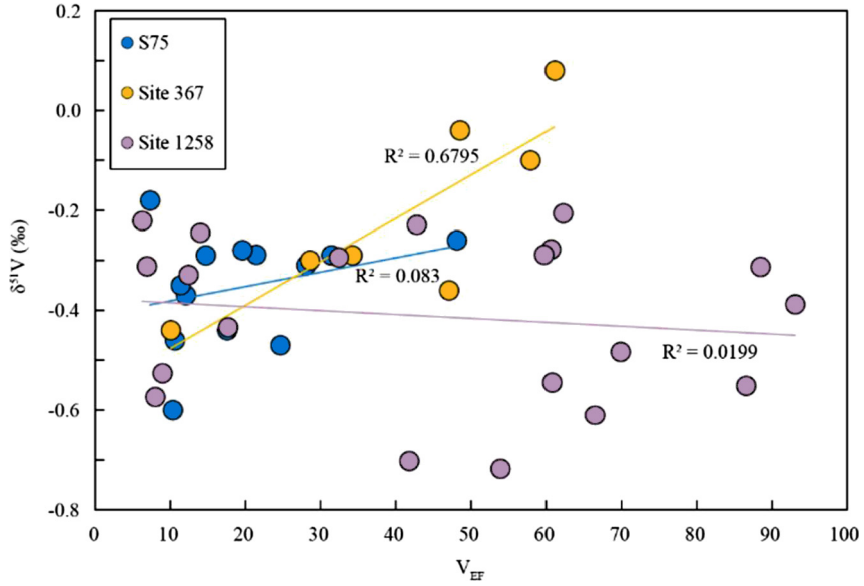

Fig. 3. The regression analysis between sedimentary V enrichment factors (V_{EF}) and $\delta^{51}V$ values.

$$M_{V\_t} = M_{V\_m} \cdot \left(\frac{F_{ri}}{\sum_{sink_i} F_{i\_m} \cdot \frac{A_{i\_t}}{A_{i\_m}}} \right)^{\frac{1}{\alpha_i}} = \frac{M_{V\_m}}{\left(\sum_{sink_i} f_{i\_m} \cdot \frac{A_{i\_t}}{A_{i\_m}} \right)^{\frac{1}{\alpha_i}}} \tag{11}$$

And the proportion of the sink f_i under the new steady state would be:

$$f_{i\_t} = \frac{F_{i\_t}}{F_{ri}} = \frac{F_{i\_m}}{F_{ri}} \cdot \frac{A_{i\_t}}{A_{i\_m}} \cdot \left(\frac{M_{V\_t}}{M_{V\_m}} \right)^{\alpha_i} = f_{i\_m} \cdot \frac{A_{i\_t}}{A_{i\_m}} \cdot \left(\frac{M_{V\_t}}{M_{V\_m}} \right)^{\alpha_i} \tag{12}$$

Then, the seawater $\delta^{51}V$ value under the new steady state can be calculated with equation (2).

The coefficient α_i reflects the sensitivity of the sinks to the marine V reservoir size, with larger values indicating greater sensitivities of the sinks to the seawater [V], namely, along with the expanding of the oceanic anoxia/euxinia, the new mass balance state can be achieved with a smaller decreasing magnitude of the marine V reservoir size. The sensitivity test shows that α_i can affect the magnitude of the perturbation to the marine V reservoir size in response to the expansion of reducing conditions over the seafloor but will not change the proportional distributions of the sinks and the seawater $\delta^{51}V$ values (Fig. 4, S1 and S2). The observations of the sedimentary enrichment of trace metals (Algeo and Rowe, 2012) in modern marine depositional environments suggest a linear control from the marine element reservoir size, thus, it is more reasonable to set $\alpha_i = 1$. The results show that, with the expansion of the anoxic area, the proportion of the anoxic sink will quickly increase, and the marine V reservoir size is remarkably shrunk by as much as ~80%, whereas the contemporaneous seawater $\delta^{51}V$ value only shifts to ~0.05‰ which is analytically indistinguishable from the modern seawater $\delta^{51}V$ range of 0.20 ± 0.15‰ (2SD) (Fig. 4A and 4C, Wu et al., 2019a). In contrast, the expansion of the oceanic euxinia and the subsequent intensified burial of V in euxinic sediments can result in greater seawater $\delta^{51}V$ perturbation at the smaller sacrifice of the marine V reservoir (Fig. 4B and 4D).

Therefore, based on the above discussion, we infer that the contemporaneous seawater $\delta^{51}V$ values in the proto-North Atlantic Ocean throughout OAE-2 were likely similar to or analytically indistinguishable from the modern open ocean values (0.20 ± 0.15‰ (2SD), Wu et al., 2019a). Thus, changes in the baseline of seawater values throughout this event likely do not control the observed variations and could only be a secondary influence on the observed values and trends.

4.2. Variable bottom water redox fluctuations at site 1258

The distribution of Fe species in sediments at Site 1258 indicates persistent euxinic bottom water conditions for the investigated stratigraphic section (420-430 m, Owens et al., 2016), and such a scenario is also suggested by the high organic matter S/C ratios which require shoaling euxinic conditions into the shallow portion of the water columns and rapid sulfurization of fresh organic matter (Raven et al., 2019). Discordant with the geochemical proxies, the paleontological evidence indicates fluctuating redox conditions in bottom waters for the pre-OAE-2 section (below 426 m) between the anoxic conditions as indicated by scarce benthic foraminifers and the hypoxic conditions which allowed for increasing abundance and diversity of the low-oxygen-tolerant benthic foraminifers (Friedrich et al., 2006). For the OAE-2 section (422-426 m), the bottom waters presented more stable anoxic conditions with transient recovery to weak oxygenation as revealed by the occasional appearance of benthic foraminifers (Fig. 5, Friedrich et al., 2006). The anoxic conditions lingered for the post-OAE-2 section (420-422 m) as indicated by the scarce of benthic foraminifers, supporting benthic foraminiferal evidence that reoxygenation of the seafloor occurred approximately 500 kyrs after OAE-2 (Friedrich et al., 2006). Similarly, the sedimentary $\delta^{51}V$ profile at Site 1258 presents considerable variations which plot in the hypoxic-to-euxinic regime throughout OAE-2, assuming consistent $\Delta_{sw\text{-}sink}$ values and the contemporaneous seawater $\delta^{51}V$ values similar to modern oceans as aforementioned (Fig. 2C). To further test the responses of the sedimentary $\delta^{51}V$ signatures to bottom water hypoxic-to-anoxic fluctuations, we compare the sedimentary $\delta^{51}V$ variations with the distributions of the low-oxygen-tolerant benthic foraminifera taxa, *Gavelinella spp*., which are shown to be able to survive as the opportunists that quickly repopulate the low-oxygen environments as one of the first species (e.g., Friedrich et al., 2005). Importantly, the pre-OAE-2 sediments with relatively abundant presence of *Gavelinella spp*. foraminifers (~10 to > 100 individuals/g in sediments) coincide with the negative perturbations of the sedimentary $\delta^{51}V$ values less than ~-0.50‰, suggesting relatively oxic bottom water conditions (Fig. 5). During OAE-2,

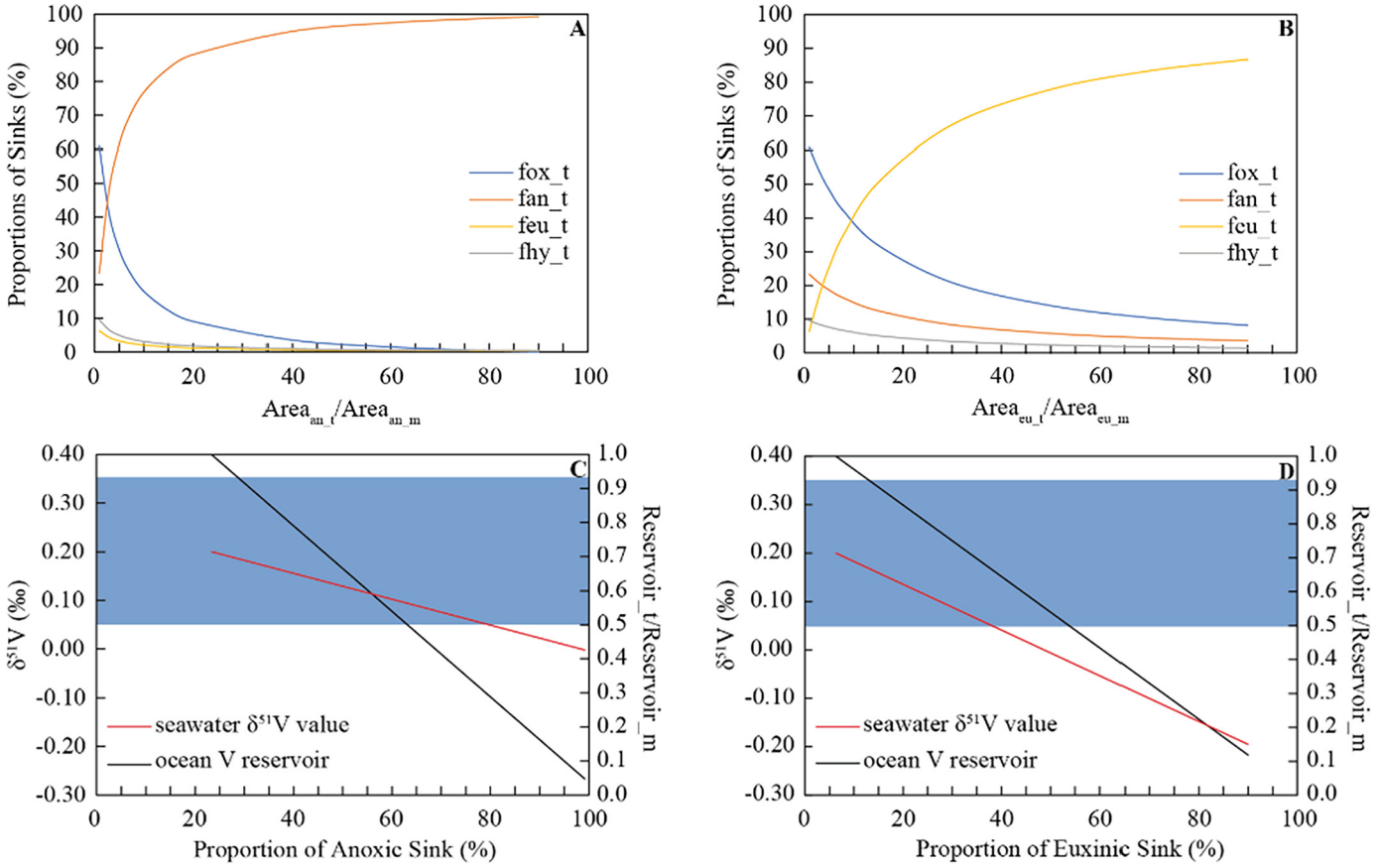

Fig. 4. The coefficient α_i is set as 1. Panel A and panel B, respectively, indicate the proportional distributions of the four sinks, i.e., the oxic sink (ox), the anoxic sink (an), the euxinic sink (eu), and the hydrothermal sink (hy) along with the expansion of the anoxic area (A) and the euxinic area (B) over the seafloor. The subscript m denotes the modern values and the subscript t indicates values during the expansion of the oceanic anoxia/euxinia. Panel C and panel D illustrate the marine V reservoir size and the seawater δ^{51}V signature in response to the expansion of oceanic anoxia (C) and euxinia (D). The blue bar denotes the modern seawater δ^{51}V range (Wu et al., 2019a).

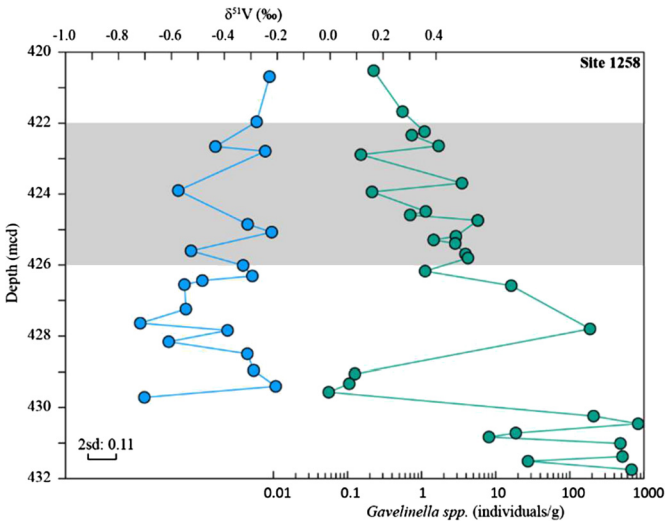

Fig. 5. The comparison of the sedimentary δ^{51}V profile (the long-term in-lab 2SD is 0.11‰) and the abundances of the *Gavelinella spp*. benthic foraminifers for Site 1258. The grey bar indicates the duration of OAE-2 as constrained by the positive CIE.

the sharp decreasing even vanishing of *Gavelinella spp*. foraminifers proposes the development of more intense and stable anoxic conditions in bottom waters, which was occasionally interrupted by weak reoxygenation as indicated by the sporadic reappearance of *Gavelinella spp*. foraminifers and the negative perturbations of the sedimentary δ^{51}V values (Fig. 5).

Hence, to reconcile current geochemical and paleontological evidence, we propose refining the spatiotemporal structure of redox conditions at Demerara Rise throughout OAE-2. Rather than the previous idea that redox conditions were dominantly euxinic and non-variant, there was likely a strongly reducing anoxic/euxinic wedge that impinged onto the shallower zone throughout OAE-2, which allowed for the formation of sulfides and quick sulfurization of organic matter (Raven et al., 2019). The variable bottom water redox conditions in deeper waters were likely influenced by the expansion/retreat of this anoxic/euxinic zone that was much like modern oxygen minimum zones (Fig. 6A and 6B, Friedrich et al., 2006). During the expansion periods of the anoxic/euxinic zone, the benthic foraminifers vanished due to the intense bottom water anoxic conditions. In contrast, during the retreating periods when the anoxic/euxinic zone was constrained to the shallower shelf and the anoxic conditions were constrained below the sediment-water interface, the low-oxygen-tolerant benthic foraminifers could still live in the weakly-oxygenated deeper water below the anoxic/euxinic wedge while pyrites and sulfurized organic particulates formed in the shallower zone could persist through such depositional environments, particularly with relatively high burial rates (i.e., burial rates at marginal settings) of ~1 cm/kyr at Site 1258 during the CIE portion of the section as estimated with a linear sedimentation rate model (Erbacher et al., 2005; Owens et al., 2016).

5. Conclusions

For the first time, we applied the sedimentary δ^{51}V values of black shales at three sites in the proto-North Atlantic Basin

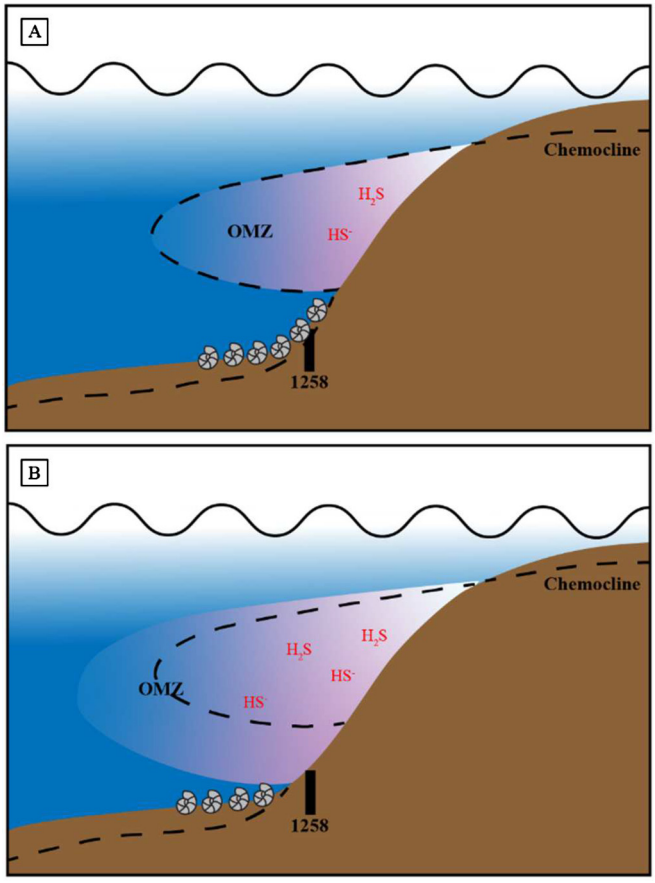

Fig. 6. Local conceptual model for Demerara Rise with oscillating anoxic/euxinic wedge impinged onto the shallower slope and/or fluctuating anoxic conditions (below the dashed line) in pore fluids at Site 1258 throughout OAE-2. Panel A indicates a "retreating" anoxic/euxinic wedge constrained in shallower areas and/or the anoxic conditions constrained within the pore fluids. Panel B indicates an "expanding" anoxic/euxinic wedge to deeper areas and/or shoaling of the anoxic conditions in pore fluids.

throughout OAE-2. No obvious stratigraphic trends emerge from the three sedimentary δ^{51}V profiles throughout OAE-2, which suggests limited perturbation to the global contemporaneous seawater δ^{51}V values. Instead, the sedimentary δ^{51}V variations predominantly respond to variable local bottom water redox fluctuations at the three sites despite the general global expansion of oceanic anoxia/euxinia as indicated by global proxy records. Furthermore, the sedimentary δ^{51}V values under the relatively stable anoxic-to-euxinic conditions at Well S75 and Site 367 are analogous to values recorded in modern anoxic-to-euxinic environments, suggesting the seawater δ^{51}V values of the proto-North Atlantic Ocean throughout OAE-2 comparable to the modern seawater δ^{51}V values. In contrast, Site 1258 presents more variable sedimentary δ^{51}V values that covary with the abundances of the low-oxygen-tolerant benthic foraminifera taxa with the negative perturbations of the sedimentary δ^{51}V values indicating transient weakly-oxygenated bottom waters that allowed for the reappearance of opportunistic benthic foraminifers.

This study has provided a framework further testing the V isotope system, as a novel redox proxy, to track bottom water redox fluctuations in a well-sampled and -studied interval of time. Importantly, this work provides a unique and new geochemical record for short-term weak oxygenation in bottom waters which corresponds to the previous paleontological evidence for small redox variations. Vanadium isotopes could be utilized to better constrain the bottom water redox variations, thus providing better constraints on the temporal redox evolutions of the ancient oceans that impact related biogeochemical cycles and radiation/extinction events.

CRediT authorship contribution statement

Siqi Li: Investigation, Methodology, Validation, Visualization, Writing – original draft. **Oliver Friedrich:** Investigation, Methodology, Writing – review & editing. **Sune G. Nielsen:** Writing – review & editing. **Fei Wu:** Methodology, Writing – review & editing. **Jeremy D. Owens:** Conceptualization, Funding acquisition, Supervision, Writing – review & editing.

Declaration of competing interest

The authors declare that they have no known competing financial interests or personal relationships that could have appeared to influence the work reported in this paper.

Data availability

Data will be made available on request.

Acknowledgements

We thank G. White for instrumentation troubleshooting at the National High Magnetic Field Laboratory. This work was funded by grants from NASA Exobiology 80NSSC18K1532 (JDO), Alfred P. Sloan Foundation FG-2020-13552 (JDO), and the FSU EOAS Winchester Fund for graduate student support (SL). The lab is supported by the National High Magnetic Field Laboratory (Tallahassee, Florida), which is funded by the National Science Foundation Cooperative Agreement No. DMR1644779 and the State of Florida.

Appendix A. Supplementary material

Supplementary material related to this article can be found online at https://doi.org/10.1016/j.epsl.2023.118237.

References

Adams, D.D., Hurtgen, M.T., Sageman, B.B., 2010. Volcanic triggering of a biogeochemical cascade during Oceanic Anoxic event 2. Nat. Geosci. 3, 201–204.
Algeo, T.J., 2004. Can marine anoxic events draw down the trace element inventory of seawater? Geology 32, 1057–1060.
Algeo, T.J., Lyons, T.W., 2006. Mo–total organic carbon covariation in modern anoxic marine environments: implications for analysis of paleoredox and paleohydrographic conditions. Paleoceanography 21.
Algeo, T.J., Rowe, H., 2012. Paleoceanographic applications of trace-metal concentration data. Chem. Geol. 324–325, 6–18.
Berrocoso, Á.J., MacLeod, K.G., Calvert, S.E., Elorza, J., 2008. Bottom water anoxia, inoceramid colonization, and benthopelagic coupling during black shale deposition on Demerara Rise (late Cretaceous western tropical North Atlantic). Paleoceanography 23.
Boyer, D.L., Owens, J.D., Lyons, T.W., Droser, M.L., 2011. Joining forces: combined biological and geochemical proxies reveal a complex but refined high-resolution palaeo-oxygen history in Devonian epeiric seas. Palaeogeogr. Palaeoclimatol. Palaeoecol. 306, 134–146.
Chen, X., et al., 2022. Iron and manganese shuttle has no effect on sedimentary thallium and vanadium isotope signatures in Black Sea sediments. Geochim. Cosmochim. Acta 317, 218–233.
Clarkson, M.O., et al., 2018. Uranium isotope evidence for two episodes of deoxygenation during Oceanic Anoxic event 2. Proc. Natl. Acad. Sci. 115, 2918–2923.
Cole, D.B., Zhang, S., Planavsky, N.J., 2017. A new estimate of detrital redox-sensitive metal concentrations and variability in fluxes to marine sediments. Geochim. Cosmochim. Acta 215, 337–353.
Collier, R.W., 1984. Particulate and dissolved vanadium in the North Pacific Ocean. Nature 309, 441.
Dickson, A.J., 2017. A molybdenum-isotope perspective on Phanerozoic deoxygenation events. Nat. Geosci. 10, 721–726.
Dickson, A.J., Jenkyns, H.C., Porcelli, D., van den Boorn, S., Idiz, E., 2016. Basin-scale controls on the molybdenum-isotope composition of seawater during Oceanic Anoxic event 2 (late Cretaceous). Geochim. Cosmochim. Acta 178, 291–306.

Dong, L.H., et al., 2021. Determination of vanadium isotope compositions in carbonates using an Fe coprecipitation method and MC-ICP-MS. Anal. Chem. 93, 7172–7179.
Du Vivier, A.D.C., et al., 2014. Marine 187Os/188Os isotope stratigraphy reveals the interaction of volcanism and ocean circulation during Oceanic Anoxic event 2. Earth Planet. Sci. Lett. 389, 23–33.
Einsele, G., Wiedmann, J., 1982. Turonian black shales in the Moroccan Coastal basins: first upwelling in the Atlantic Ocean? In: von Rad, U., Hinz, K., Sarnthein, M., Seibold, E. (Eds.), Geology of the Northwest African Continental Margin. Springer, pp. 396–414.
Elrick, M., Molina-Garza, R., Duncan, R., Snow, L., 2009. C-isotope stratigraphy and paleoenvironmental changes across OAE2 (mid-Cretaceous) from shallow-water platform carbonates of southern Mexico. Earth Planet. Sci. Lett. 277, 295–306.
Erbacher, J., Mosher, D., Malone, M., ODP Leg 207 Scientific Party, 2004. Drilling probes past carbon cycle perturbations on the Demerara Rise. Eos Trans. AGU 85, 57–63.
Erbacher, J., Friedrich, O., Wilson, P.A., Birch, H., Mutterlose, J., 2005. Stable organic carbon isotope stratigraphy across Oceanic Anoxic event 2 of Demerara Rise, western tropical Atlantic. Geochem. Geophys. Geosyst. 6.
Fan, H., Ostrander, C.M., Auro, M., Wen, H., Nielsen, S.G., 2021. Vanadium isotope evidence for expansive ocean euxinia during the appearance of early Ediacara biota. Earth Planet. Sci. Lett. 567, 117007.
Friedrich, O., Nishi, H., Pross, J., Schmiedl, G., Hemleben, C., 2005. Millennial- to Centennial-Scale Interruptions of the Oceanic Anoxic event 1b (Early Albian, mid-Cretaceous) inferred from Benthic Foraminiferal Repopulation events. Palaios 20, 64–77.
Friedrich, O., Erbacher, J., Mutterlose, J., 2006. Paleoenvironmental changes across the Cenomanian/turonian boundary event (Oceanic Anoxic event 2) as indicated by benthic foraminifera from the Demerara Rise (ODP leg 207). Rev. Micropaléontol. 49, 121–139.
Hastings, D.W., Emerson, S.R., Erez, J., Nelson, B.K., 1996. Vanadium in foraminiferal calcite: evaluation of a method to determine paleo-seawater vanadium concentrations. Geochim. Cosmochim. Acta 60, 3701–3715.
Heard, A.W., et al., 2023. Coupled vanadium and thallium isotope constraints on Mesoproterozoic ocean oxygenation around 1.38-1.39 Ga. Earth Planet. Sci. Lett. 610, 118127.
Herrle, J.O., Pross, J., Friedrich, O., Kößler, P., Hemleben, C., 2003. Forcing mechanisms for mid-Cretaceous black shale formation: evidence from the Upper Aptian and Lower Albian of the Vocontian Basin (SE France). Palaeogeogr. Palaeoclimatol. Palaeoecol. 190, 399–426.
Ho, P., Lee, J.M., Heller, M.I., Lam, P.J., Shiller, A.M., 2018. The distribution of dissolved and particulate Mo and V along the U.S. GEOTRACES East Pacific Zonal Transect (GP16): the roles of oxides and biogenic particles in their distributions in the oxygen deficient zone and the hydrothermal plume. Mar. Chem. 201, 242–255.
Hofmann, A.F., Peltzer, E.T., Walz, P.M., Brewer, P.G., 2011. Hypoxia by degrees: establishing definitions for a changing ocean. Deep-Sea Res., Part 1, Oceanogr. Res. Pap. 58, 1212–1226.
Jenkyns, H.C., 2010. Geochemistry of oceanic anoxic events. Geochem. Geophys. Geosyst. 11.
Kendall, B., Dahl, T.W., Anbar, A.D., 2017. The stable isotope geochemistry of Molybdenum. Rev. Mineral. Geochem. 82, 683–732.
Knežević, L., Omanović, D., Bačić, N., Mandić, J., Bura-Nakić, E., 2021. Redox speciation of vanadium in estuarine waters using improved methodology based on anion exchange chromatography coupled to HR ICP-MS system. Molecules 26, 2436.
Kolonic, S., et al., 2005. Black shale deposition on the northwest African Shelf during the Cenomanian/Turonian oceanic anoxic event: climate coupling and global organic carbon burial. Paleoceanography 20.
Kuhnt, W., Nederbragt, A., Leine, L., 1997. Cyclicity of Cenomanian-Turonian organic-carbon-rich sediments in the Tarfaya Atlantic Coastal Basin (Morocco). Cretac. Res. 18, 587–601.
Kuhnt, W., Luderer, F., Nederbragt, S., Thurow, J., Wagner, T., 2005. Orbital-scale record of the late Cenomanian-Turonian oceanic anoxic event (OAE-2) in the Tarfaya Basin (Morocco). Int. J. Earth Sci. 94, 147–159.
Kuypers, M.M.M., Pancost, R.D., Nijenhuis, I.A., Damsté, J.S.S., 2002. Enhanced productivity led to increased organic carbon burial in the euxinic North Atlantic basin during the late Cenomanian oceanic anoxic event. Paleoceanography 17, 3-1–3-13.
Levin, L.A., et al., 2009. Effects of natural and human-induced hypoxia on coastal benthos. Biogeosciences 6 (10), 2063–2098.
Lewan, M.D., Maynard, J.B., 1982. Factors controlling enrichment of vanadium and nickel in the bitumen of organic sedimentary rocks. Geochim. Cosmochim. Acta 46, 2547–2560.
Li, L., et al., 2021. Enrichment of trace metals (V, Cu, Co, Ni, and Mo) in Arctic Sediments—from Siberian Arctic shelves to the Basin. J. Geophys. Res., Oceans 126, e2020JC016960.
Liu, J., Algeo, T.J., 2020. Beyond redox: control of trace-metal enrichment in anoxic marine facies by watermass chemistry and sedimentation rate. Geochim. Cosmochim. Acta 287, 296–317.
Lyons, T.W., Severmann, S., 2006. A critical look at iron paleoredox proxies: new insights from modern euxinic marine basins. Geochim. Cosmochim. Acta 70, 5698–5722.
Middelburg, J.J., Levin, L.A., 2009. Coastal hypoxia and sediment biogeochemistry. Biogeosciences 6, 1273–1293.
Nielsen, S.G., 2020. Vanadium isotopes: a proxy for ocean oxygen variations. Elem. Geochem. Tracers Earth Syst. Sci.
Nielsen, S.G., Prytulak, J., Halliday, A.N., 2011. Determination of precise and accurate 51V/50V isotope ratios by MC-ICP-MS, Part 1: chemical separation of vanadium and mass spectrometric protocols. Geostand. Geoanal. Res. 35, 293–306.
Nielsen, S.G., Owens, J.D., Horner, T.J., 2016. Analysis of high-precision vanadium isotope ratios by medium resolution MC-ICP-MS. J. Anal. At. Spectrom. 31, 531–536.
Ostrander, C.M., Owens, J.D., Nielsen, S.G., 2017. Constraining the rate of oceanic deoxygenation leading up to a Cretaceous Oceanic Anoxic event (OAE-2: ∼94 Ma). Sci. Adv. 3, e1701020.
Owens, J.D., et al., 2012. Iron isotope and trace metal records of iron cycling in the proto-North Atlantic during the Cenomanian-Turonian Oceanic Anoxic event (OAE-2). Paleoceanography 27.
Owens, J.D., et al., 2013. Sulfur isotopes track the global extent and dynamics of euxinia during Cretaceous Oceanic Anoxic event 2. Proc. Natl. Acad. Sci. 110, 18407–18412.
Owens, J.D., Reinhard, C.T., Rohrssen, M., Love, G.D., Lyons, T.W., 2016. Empirical links between trace metal cycling and marine microbial ecology during a large perturbation to Earth's carbon cycle. Earth Planet. Sci. Lett. 449, 407–417.
Pogge von Strandmann, P.A.E., Jenkyns, H.C., Woodfine, R.G., 2013. Lithium isotope evidence for enhanced weathering during Oceanic Anoxic event 2. Nat. Geosci. 6, 668–672.
Poulton, S.W., Canfield, D.E., 2011. Ferruginous conditions: a dominant feature of the ocean through Earth's history. Elements 7, 107–112.
Poulton, S.W., et al., 2015. A continental-weathering control on orbitally driven redox-nutrient cycling during Cretaceous Oceanic Anoxic event 2. Geology 43, 963–966.
Qi, Y.H., et al., 2022. Coupled variations in V-Fe abundances and isotope compositions in latosols: implications for V mobilization during chemical weathering. Geochim. Cosmochim. Acta 320, 26–40.
Raiswell, R., et al., 2018. The iron paleoredox proxies: a guide to the pitfalls, problems and proper practice. Am. J. Sci. 318, 491–526.
Raven, M.R., et al., 2019. Paired organic matter and pyrite δ34S records reveal mechanisms of carbon, sulfur, and iron cycle disruption during Ocean Anoxic event 2. Earth Planet. Sci. Lett. 512, 27–38.
Reinhard, C.T., et al., 2013. Proterozoic ocean redox and biogeochemical stasis. Proc. Natl. Acad. Sci. 110, 5357–5362.
Rudnick, R.L., Gao, S., 2003. Composition of the continental crust. Treatise Geochem. 3, 659.
Scholz, F., et al., 2011. Early diagenesis of redox-sensitive trace metals in the Peru upwelling area – response to ENSO-related oxygen fluctuations in the water column. Geochim. Cosmochim. Acta 75, 7257–7276.
Schuth, S., et al., 2019. Vanadium and its isotope composition of river water and seawater: analytical improvement and implications for vanadium isotope fractionation. Chem. Geol. 528, 119261.
Shiller, A.M., Mao, L., 2000. Dissolved vanadium in rivers: effects of silicate weathering. Chem. Geol. 165, 13–22.
Sinninghe Damsté, J.S., Köster, J., 1998. A euxinic southern North Atlantic Ocean during the Cenomanian/Turonian oceanic anoxic event. Earth Planet. Sci. Lett. 158, 165–173.
Sturdivant, S.K., Díaz, R.J., Cutter, G.R., 2012. Bioturbation in a declining oxygen environment, in situ observations from Wormcam. PLoS ONE 7, e34539.
Trefry, J.H., Metz, S., 1989. Role of hydrothermal precipitates in the geochemical cycling of vanadium. Nature 342, 531–533.
Tribovillard, N., Algeo, T.J., Lyons, T., Riboulleau, A., 2006. Trace metals as paleoredox and paleoproductivity proxies: an update. Chem. Geol. 232, 12–32.
Wang, D., Sañudo Wilhelmy, S.A., 2009. Vanadium speciation and cycling in coastal waters. Mar. Chem. 117, 52–58.
Wanty, R.B., Goldhaber, M.B., 1992. Thermodynamics and kinetics of reactions involving vanadium in natural systems: accumulation of vanadium in sedimentary rocks. Geochim. Cosmochim. Acta 56, 1471–1483.
Wehrli, B., Stumm, W., 1989. Vanadyl in natural waters: adsorption and hydrolysis promote oxygenation. Geochim. Cosmochim. Acta 53, 69–77.
Wei, W., et al., 2023. Vanadium isotope evidence for widespread marine oxygenation from the late Ediacaran to early Cambrian. Earth Planet. Sci. Lett. 602, 117942.
Westermann, S., Vance, D., Cameron, V., Archer, C., Robinson, S.A., 2014. Heterogeneous oxygenation states in the Atlantic and tethys oceans during Oceanic Anoxic event 2. Earth Planet. Sci. Lett. 404, 178–189.
Wu, F., et al., 2015. First-principles investigation of vanadium isotope fractionation in solution and during adsorption. Earth Planet. Sci. Lett. 426, 216–224.
Wu, F., et al., 2016. Vanadium isotope measurement by MC-ICP-MS. Chem. Geol. 421, 17–25.
Wu, F., et al., 2019a. Vanadium isotope composition of seawater. Geochim. Cosmochim. Acta 244, 403–415.

Wu, F., Owens, J.D., Tang, L., Dong, Y., Huang, F., 2019b. Vanadium isotopic fractionation during the formation of marine ferromanganese crusts and nodules. Geochim. Cosmochim. Acta 265, 371–385.
Wu, F., et al., 2020. Sedimentary vanadium isotope signatures in low oxygen marine conditions. Geochim. Cosmochim. Acta 284, 134–155.
Wu, F., Owens, J.D., German, C.R., Mills, R.A., Nielsen, S.G., 2022. Vanadium isotope fractionation during hydrothermal sedimentation: implications for the vanadium cycle in the oceans. Geochim. Cosmochim. Acta 328, 168–184.
Zhang, F., et al., 2020. Uranium isotopes in marine carbonates as a global ocean paleoredox proxy: a critical review. Geochim. Cosmochim. Acta 287, 27–49.